High breakdown single-crystal GaN p-n diodes by molecular beam epitaxy

Meng Qi,[1] Kazuki Nomoto,[1,2] Mingda Zhu,[1,2] Zongyang Hu,[1,2] Yuning Zhao,[1] Vladimir Protasenko,[1,2] Bo Song,[1,2] Xiaodong Yan,[1] Guowang Li,[1] Jai Verma,[1] Samuel Bader,[2] Patrick Fay,[1] Huili Grace Xing,[1,2] and Debdeep Jena[1,2,a)]
[1]*Department of Electrical Engineering, University of Notre Dame, Notre Dame, Indiana 46556, USA*
[2]*Departments of ECE and MSE, Cornell University, Ithaca, New York 14853, USA*

(Received 13 October 2015; accepted 19 November 2015; published online 8 December 2015)

Molecular beam epitaxy grown GaN p-n vertical diodes are demonstrated on single-crystal GaN substrates. A low leakage current $<3\,\text{nA/cm}^2$ is obtained with reverse bias voltage up to $-20\,\text{V}$. With a 400 nm thick n-drift region, an on-resistance of $0.23\,\text{m}\Omega\,\text{cm}^2$ is achieved, with a breakdown voltage corresponding to a peak electric field of ~3.1 MV/cm in GaN. Single-crystal GaN substrates with very low dislocation densities enable the low leakage current and the high breakdown field in the diodes, showing significant potential for MBE growth to attain near-intrinsic performance when the density of dislocations is low. © *2015 AIP Publishing LLC*.
[http://dx.doi.org/10.1063/1.4936891]

The wide bandgap III-nitride semiconductors have enabled several new applications in high-speed transistors[1–4] and in visible and short-wavelength light emitting diodes and lasers.[5,6] Due to the high breakdown electric field $E_{br} \sim 3.5$ MV/cm and high electron mobilities $\mu_n \sim 1000\,\text{cm}^2/\text{V s}$, GaN has recently drawn special attention for electronic devices that require energy-efficient high power and high voltage rectification and switching.[7–9] Lateral high-voltage transistors using GaN HEMTs on silicon support the high voltage by making the gate-drain separation large: this requires a large footprint area. Using vertical device geometries enables an efficient use of the wafer area by redirecting the high voltage drop into the bulk of the wafer. Furthermore, in unipolar lateral devices such as HEMTs, the "breakdown" is typically not due to intrinsic avalanche mechanisms, but due to gate leakage or allied processes, which do not utilize the entire bandgap of GaN. Vertical p-n junctions allow reaching the intrinsic capabilities of a material, thus allowing high breakdown voltage and low on-resistance (R_{on}), and are expected to lead to superior energy-efficient three-terminal GaN power switches. High-voltage vertical GaN diodes have long been challenging due to the lack of low dislocation density substrates. Threading dislocations (TDs) that propagate through the epitaxial layers in the active regions act as current short paths and increase the off-state leakage, degrading the breakdown properties.

Recently, high-quality single crystal GaN substrates with low dislocation densities have become available. These substrates have enabled epitaxial growth of GaN vertical p-n junctions by metal-organic chemical vapor deposition (MOCVD).[10,11] Previous work of MBE grown GaN vertical p-n junctions by *ammonia* MBE demonstrated low-leakage diodes.[12] But no MBE work—be it using ammonia or plasma nitrogen—has demonstrated high voltage or high power p-n junction diodes where thick drift layers are necessary. MBE enables a high degree of control of alloy compositions, high quality AlN layers and heterostructures, and efficient (Mg) acceptor doping for buried p-type layers that do not require activation annealing. This is a unique advantage over MOCVD for several devices. Furthermore, recent reports of very high growth rates by plasma MBE make the technique attractive for throughput considerations.[13] Taking advantage of single-crystal low-dislocation density bulk GaN substrates, we show in this work that RF plasma MBE grown p-n junctions can attain near-intrinsic behavior. GaN vertical p-n junctions with off-state leakage current as low as $3\,\text{nA/cm}^2$, breakdown field $E_{br} \sim 3.1$ MV/cm, and $R_{on} \sim 0.23\,\text{m}\Omega\,\text{cm}^2$ are achieved in epitaxial diodes. These breakdown and leakage characteristics represent the highest performance metrics in GaN p-n junction diodes grown by MBE.

Structurally identical p-n junctions were grown by MBE on three different metal-polar GaN substrates whose specifications are shown in Table I. All three substrates are heavily n-doped, which enables back-side ohmic metal contacts. The key difference of the three substrates is the TD densities. The TD densities of $1–2 \times 10^7\,\text{cm}^{-3}$, $2–5 \times 10^5\,\text{cm}^{-3}$, and $5 \times 10^4\,\text{cm}^{-3}$ are measured by the etch pit density (EPD) method for substrates *A*, *B*, and *C*, respectively. For the "epi-ready" substrates from vendor, we performed *ex situ* and *in situ* cleaning before the growth. Before loading the samples into the MBE system, the substrates are first cleaned in solvents (acetone, methanol, and isopropanol, respectively) under ultrasonication to remove surface contaminants. The substrates are then mounted on silicon wafers with indium and loaded into the MBE system. Once loaded, the substrates are outgassed at 200 °C for more than 7 h (typically overnight) in the load-lock chamber. Then, the substrates are transferred to a buffer chamber, where the samples are further baked at 400 °C for ~2 h for further degassing. Finally, the samples are transferred into the growth chamber to perform epitaxial growth. Once the substrate reaches the growth temperature, a 30 s Ga flux soak is usually used to guarantee a Ga-rich surface, before commencing with homoepitaxial growth. The MBE growth conditions for the device active layers were identical for the samples.

A 400-nm-thick lightly Si-doped GaN layer was grown at a substrate temperature of 720 °C under a Ga flux of

a)Electronic mail: djena@cornell.edu

TABLE I. Substrates specifications for MBE grown p-n junctions. σ: carrier concentration, μ: carrier mobility, t: thickness, TD: threading dislocation density, and ρ: resistivity at 300 K.

GaN Substrate	σ (cm^{-3})	μ (cm^2/V s)	t (μm)	ρ (mΩ cm)	TD (cm^{-2})
A	$\sim 4 \times 10^{18}$	107	300 ± 50	10.9 ± 1.8	$1–2 \times 10^7$
B	$\sim 3 \times 10^{18}$	211	290	7.2	$2–5 \times 10^5$
C	$\sim 10^{19}$	150	566	2.7	$< 5 \times 10^4$

1.6×10^{-7} Torr by plasma-assisted MBE in a Veeco Gen930 system. The RF power of the nitrogen plasma was kept at 200 W for the entire growth, and the corresponding growth rate was ~180 nm/h. The growth was performed under slightly metal-rich conditions to ensure step-flow. Because the breakdown voltage is very sensitive to the doping density, the unintentional doping (UID) density needs to be carefully controlled. In order to achieve low n-type doping in this study, the Mg cell and Al cell were kept at standby temperatures (Mg ~ 200 °C and Al ~ 800 °C) to minimize oxygen outgassing, because oxygen is a donor dopant in GaN. For the 400-nm-thick drift layer, the Si doping concentration was $N_D = 1 \sim 2 \times 10^{17}\,cm^{-3}$. After the growth of the 400-nm-thick n-GaN layer, the Si shutter was closed, and a 10-nm-thick UID GaN layer was grown. During the growth of the UID GaN layer, the substrate temperature was ramped down from 720 °C to 600 °C, and the Mg cell temperature was simultaneously ramped up from 200 °C to 400 °C for the growth of the subsequent acceptor-doped p-type GaN layer. This process allowed the growth of a 100-nm-thick p-GaN layer with Mg doping concentration of $N_A \sim 2 \times 10^{19}\,cm^{-3}$ without any growth interruption. A ~20 nm thick heavily doped p + GaN cap layer with $N_A \sim 10^{20}\,cm^{-3}$ was grown to facilitate Ohmic contacts.

A schematic cross-section of a fabricated GaN vertical p-n diode is shown Fig. 1(a), and Fig. 1(b) shows the corresponding cross-section Transmission-Electron Micrograph (TEM) image of a representative device on substrate C. The TEM imaging confirmed that the MBE growth of homoepitaxial GaN p-n junction diodes is achieved without the introduction of additional dislocations. The excess gallium droplets after MBE growth were removed in HCl before device fabrication. The samples were then patterned by optical lithography and etched to >600 nm height mesa by reactive ion etching (RIE) for device isolation. For the n-type Ohmic contacts, 50/250/30 nm Ti/Al/Au stacks were evaporated on the backside of the n-type bulk samples without patterning. A second optical lithography step defined the patterns for the top p-type Ohmic contacts, for which alloyed contacts formed by E-beam evaporation of 50/50 nm Pd/Pt stacks followed by a thermal annealing in N_2 at 400 °C for 10 min were used. A metal pad stack consisting of 50/100/50 nm Ti/Al/Au was evaporated on top of the p-type Ohmic metals, respectively, to further improve the conductivity. These metal layer stacks are clearly visible in the TEM image of Fig. 1(b).

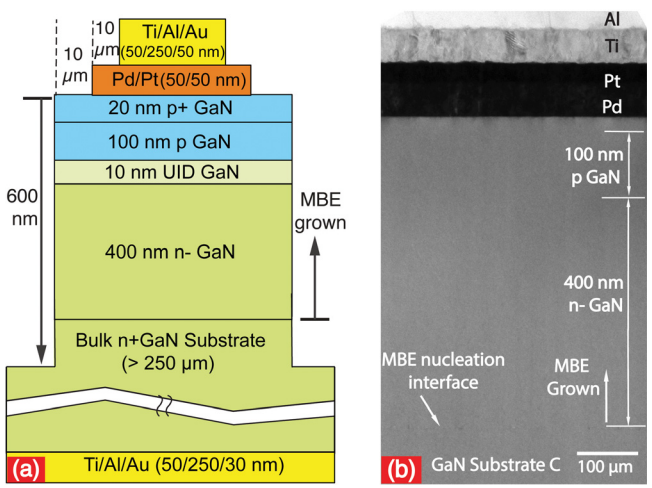

FIG. 1. (a) Schematic structure and (b) cross-section TEM of fabricated vertical MBE-grown p-n diodes on low-dislocation density bulk GaN crystal substrate C.

The measured electrical forward-bias I-V characteristics of nominally identical 70 μm diameter vertical p-n diodes on the three substrates of different dislocation densities [Table I] are shown in Figs. 2(a) and 2(b) in linear and log scales. The measurements were performed on ~30 devices on each substrate, ~100 devices in total, that enabled us to draw several conclusions. All diodes showed rectifying behavior with the turn on voltages slightly lower than the bandgap of GaN. The diodes on substrates C and A show lower on-current than B; this is attributed to different p-type Ohmic contact resistances, and is not intrinsic to the diode. The log-scale forward-bias characteristics shown in Fig. 2(b) reveals a significantly lower leakage current before turn-on for diodes on substrate C compared to the other two. This below turn-on current is also observed to decrease monotonically with dislocation density.

Visible light emission was observed from diodes on all substrates under forward bias. The measured electroluminescence (EL) spectrum for the diode on substrate B as an example is shown in Fig. 2(c) at a forward bias voltage of +5 V and an injection current density of ~330 A/cm^2. Two EL peaks at 3.2 eV and 2.2 eV are seen. For the ~3.2 eV peak, a sharp edge can be observed on the higher energy side. The origin of this photon peak at 3.2 eV is due to two reasons. The first is the recombination of injected electrons and holes in the depletion region, which emit photons of energy close to the GaN bandgap of 3.4 eV. The subsequent re-absorption of these photons in the Mg-doped rich p-cap layer, and re-emission at 3.2 eV corresponding to a conduction band-acceptor level transition because the Mg acceptor level is ~0.2 eV above the valence band produced the 3.2 eV peak. The second is from the electron overshoot into the p-region that recombines radiatively in that layer. The 2.2 eV peak is due to deep-level transitions in GaN and have been reported before.[14] For comparison, a photoluminescence (PL) spectrum of the pristine substrate B of single-crystal n + GaN is shown in Fig. 2(c), showing a band-edge peak at ~3.4 eV. The inset in Fig. 2(c) shows the visible emission during probing: the strong EL indicates high-quality material and confirms radiative recombination in the p-n junction, though the p-n junction structures studied here are designed for high breakdown and low-leakage applications. Since we can design for light to carry away a significant fraction of energy out of the diode, it can prove to be a very attractive way for device cooling in power electronics: a technique that

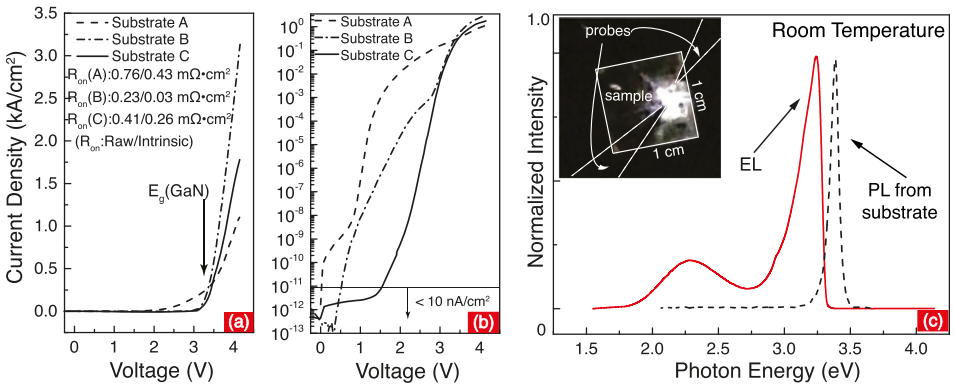

FIG. 2. Comparison of forward I-V characteristics for MBE grown p-n junctions on three different substrates plotted in (a) linear scale and (b) semilog scale. In the semilog scale, forward bias leakage currents levels of $<10\,\mathrm{nA/cm^2}$ are measured for the sample with the lowest substrate dislocation density. (c) Electroluminescence spectrum of p-n diode on substrate B, with a forward bias voltage of 5 V. A photoluminescence spectrum of the unprocessed substrate B is plotted as comparison. The inset figure shows the visible light emission during the measurement.

has not been possible in indirect bandgap power semiconductors such as Si and SiC diodes and transistors before. In an indirect bandgap semiconductor p-n diode, the entire recombination is non-radiative, leading to every electron-hole pair dumping energy equal to the bandgap into the crystal as heat. The mechanism is different in a Schottky diode (an unipolar device), because the carrier transport is by thermionic emission of electrons from the semiconductor into the metal. Thus, all the excess electron energy is dumped into the metal as heat. It is not uncommon to see degradation due to high temperature generated in the contacts. For making a three-terminal switch, the p-n diode is essential, and for both 3-terminal switches and 2-terminal diodes, if the p-n diode material is made of direct-bandgap semiconductors, it has the unique advantage of releasing the energy as light instead of heat. This may be a unique advantage of using a direct bandgap semiconductor for power electronics.

Capacitance-voltage measurements were performed on 70 μm diameter diodes grown on substrate B (as an example) at a frequency of 1 MHz, as shown in Fig. 3(a). The low leakage led to a loss tangent angle $>82°$ in the voltage range of measurement. The $1/C^2$ vs. V plot and a linear fit shown in Fig. 3(b) lets us extract an n-region doping density $N_D = 1\text{–}2 \times 10^{17}\,\mathrm{cm^{-3}}$, for the three diodes.

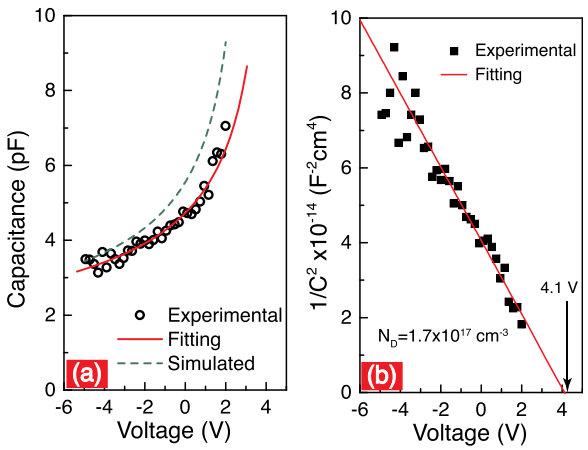

FIG. 3. (a) Capacitance-voltage characteristics from p-n diodes grown on substrate B. The measured conductance, fitting curve and the simulated curve are both plotted. (b) The $1/C^2 \sim V$ relation is plotted, and the linear fitting extracts the doping concentration in the lightly doped 400-nm-thick n-region of the p-n junction.

The donor doping densities are much lighter than the acceptor doping on the p-side ($N_A = \sim 2 \times 10^{19}\,\mathrm{cm^{-3}}$). Assuming the entire depletion region is in the n-side, we can use the relation

$$\frac{d(1/C^2)}{d(V)} = -\frac{2}{q\varepsilon_s N_D}, \quad V|_{\frac{1}{C^2}=0} = \psi_{bi} - \frac{2KT}{q}, \tag{1}$$

to extract $N_D = 1.7 \times 10^{17}\,\mathrm{cm^{-3}}$ for the representative diode on substrate B for which the data are shown in Fig. 3. The calculated C-V based on the extracted N_D is plotted in Fig. 3(a). Next, the extracted doping concentration is used to analyze the high-field behavior.

The measured reverse-bias *I-V* characteristics of the p-n diodes on the three substrates are shown in log-scale in Fig. 4(a). The reverse current density of diodes on substrate C remains lower than $\sim$nA/cm^2 for bias voltages from 2 V to -5 V. The "on/off" ratio at $\pm$ 5 V is $\sim 10^{13}$ for this diode. The diodes on substrates A and B show a significantly higher reverse leakage $\sim 1 \times 10^{-4}$ A/cm^2 in the same voltage range with an "on/off" ratio at $\pm$ 5 V of $\sim 10^8$. The reverse leakage currents correlate directly with the forward leakage currents in Fig. 2(b)—showing a very strong dependence on the dislocation density. Abrupt and catastrophic electrical breakdown was observed for all the diodes at reverse bias voltage values ranging from -20 V to -94 V, as shown in Fig. 4(a). Lower dislocation densities lead to significantly larger breakdown voltages.

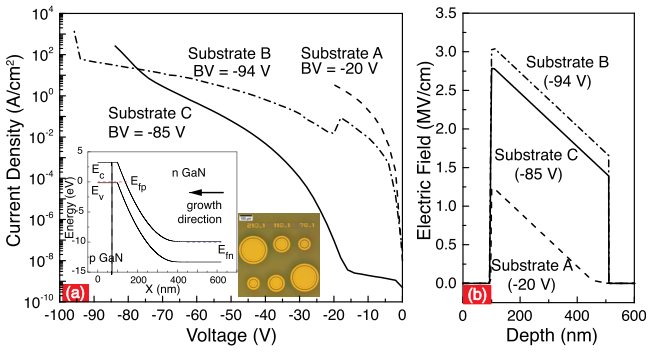

FIG. 4. (a) Semilog plot of I-V characteristics with reverse bias voltages until breakdown for three vertical GaN p-n junctions on different GaN substrates. The inset figures show the energy band diagram with -10 V bias, as well as the image of fabricated diodes under optical microscope. (b) Electric field profiles along the vertical direction of three p-n junctions on different substrates at the corresponding breakdown voltages.

The breakdown voltages are modest because the drift region is rather thin (~400 nm); it is important to investigate the electric fields. Fig. 4(b) shows the calculated electric field profile at the various breakdown voltages obtained by solving the Poisson equation. Since the doping ratio $N_A/N_D \sim 100$, the depletion region is mainly in the n-side for all junctions. For the diodes on substrates B and C, the measured *BVs* are larger than −80 V. In this case, the n-GaN region was fully depleted, as can be seen in Fig. 4(b). P-n diodes on substrate B show the highest BV of −94 V, and a corresponding electric field larger than 3.1 MV/cm at the edge of depletion region is calculated. To calculate the electric field at this breakdown voltage, $N_D = 1.7 \times 10^{17}\,\mathrm{cm}^{-3}$ is used as measured by *C-V* in Fig. 3(b). This electric field of ~3.1 MV/cm is close to the estimated critical field of 3.5–3.8 MV/cm for GaN. It is among the highest experimental results reported.[11,15–18]

For reverse bias voltages before breakdown occurs, the diodes showed increasing current density with bias. The measured data are several orders of magnitude higher than the expected current from interband Zener tunneling,[19,20] suggesting that avalanche effects, perhaps assisted by trap- and defect-assisted tunneling, are playing an important role. A mechanism of the reverse-characteristics of the bulk GaN p-n diodes is still under investigation. For now, we note that at relatively large reverse bias voltages, the diodes on substrates with lower dislocation density show lower leakage implying dislocations are significant leakage paths. Such paths associated with deep level traps-those related to dislocations have been reported.[21,22]

In summary, we have investigated the high-voltage handling capability of RF plasma-MBE grown GaN vertical p-n diodes on single-crystal GaN substrates for power diodes and switches. A very strong correlation of dislocations with both forward and reverse-bias leakage currents is observed. It is seen that plasma-MBE can attain diodes that exhibit among the highest critical breakdown fields reported till date, and leakage currents below ~nA/cm^2. This is enabled by careful control of unintentional background doping during growth. The potential for optical cooling of GaN high-voltage p-n diodes, combined with the potential of plasma MBE to grow buried p-type layers and high control of heterojunctions—especially involving AlN, and the latest developments of very high growth rates indicates that plasma MBE growth technique can make significant contributions to GaN based vertical devices for power electronics.

This work was supported by the ARPA-E SWITCHES Program and the ONR MURI program for High-Speed Electronics monitored by Dr. Paul Maki. The authors thank the Notre Dame Integrated Imaging Facility (NDIIF) for the help with the TEM measurements.

[1]U. K. Mishra, L. Shen, T. E. Kazior, and Y.-F. Wu, Proc. IEEE **96**, 287 (2008).
[2]Y. Yue, Z. Hu, J. Guo, B. Sensale-Rodriguez, G. Li, R. Wang, F. Faria, B. Song, X. Gao, S. Guo, T. Kosel, G. Snider, P. Fay, D. Jena, and H. G. Xing, Jpn. J. Appl. Phys., Part 1 **52**, 1–2 (2013).
[3]Y. Zhao, W. Chen, W. Li, M. Zhu, Y. Yue, B. Song, J. Encomendero, B. Sensale-Rodriguez, H. G. Xing, and P. Fay, Appl. Phys. Lett. **105**, 173508 (2014).
[4]D. S. Lee, X. Gao, S. Guo, D. Kopp, P. Fay, and T. Palacios, IEEE Electron Device Lett. **32**, 1525 (2011).
[5]S. Nakamura, M. Senoh, S. Nagahama, N. Iwasa, T. Yamada, T. Matsushita, H. Kiyoku, Y. Sugimoto, T. Kozaki, H. Umemoto, M. Sano, and K. Chocho, Appl. Phys. Lett. **72**, 211 (1998).
[6]Y. Taniyasu, M. Kasu, and T. Makimoto, Nature **441**, 325 (2006).
[7]J. Kuzmik, IEEE Electron Device Lett. **22**, 510 (2001).
[8]M. Zhu, B. Song, M. Qi, Z. Hu, K. Nomoto, X. Yan, Y. Cao, W. Johnson, E. Kohn, D. Jena, and H. G. Xing, IEEE Electron Device Lett. **36**, 375 (2015).
[9]R. Chu, A. Corrion, M. Chen, R. Li, D. Wong, D. Zehnder, B. Hughes, and K. Boutros, IEEE Electron Device Lett. **32**, 632 (2011).
[10]Y. Hatakeyama, K. Nomoto, N. Kaneda, T. Kawano, T. Mishima, and T. Nakamura, IEEE Electron Device Lett. **32**, 1674 (2011).
[11]I. C. Kizilyalli, A. P. Edwards, H. Nie, D. Disney, and D. Bour, IEEE Trans. Electron Devices **60**, 3067 (2013).
[12]C. A. Hurni, O. Bierwagen, J. R. Lang, B. M. McSkimming, C. S. Gallinat, E. C. Young, D. A. Browne, U. K. Mishra, and J. S. Speck, Appl. Phys. Lett. **97**, 222113 (2010).
[13]B. M. McSkimming, F. Wu, T. Huault, C. Chaix, and J. S. Speck, J. Cryst. Growth **386**, 168 (2014).
[14]I. Shalish, L. Kronik, G. Segal, Y. Rosenwaks, Y. Shapira, U. Tisch, and J. Salzman, Phys. Rev. B **59**, 9748 (1999).
[15]V. A. Dmitriev, K. G. Irvine, H. Carter, N. I. Kuznetsov, and E. V. Kalinina, Appl. Phys. Lett. **68**, 229 (1996).
[16]P. Zhao, A. Verma, J. Verma, H. Xing, and D. Jena, in CS Mantech Technical Digest 2013.
[17]A. M. Ozbek and B. J. Baliga, IEEE Electron Device Lett. **32**, 300 (2011).
[18]Y. Zhang, M. Sun, D. Piedra, M. Azize, X. Zhang, T. Fujishima, and T. Palacios, IEEE Electron Device Lett. **35**, 618 (2014).
[19]A. C. Seabaugh and Z. Qin, Proc. IEEE **98**, 2095 (2010).
[20]D. Jena, Proc. IEEE **101**, 1585 (2013).
[21]D. V. Kuksenkov, H. Temkin, A. Osinsky, R. Gaska, and M. A. Khan, Appl. Phys. Lett. **72**, 1365 (1998).
[22]P. Kozodoy, J. P. Ibbetson, H. Marchand, P. T. Fini, S. Keller, J. S. Speck, S. P. DenBaars, and U. K. Mishra, Appl. Phys. Lett. **73**, 975 (1998).